Capturing weak long-period signals: A survey of event spectra and noise threshold requirements

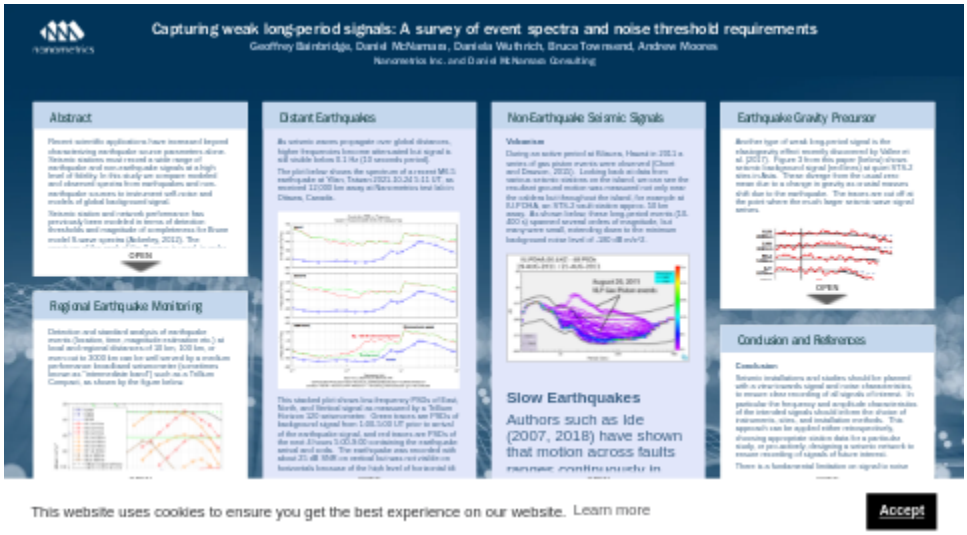

Geoffrey Bainbridge, Daniel McNamara, Daniela Wuthrich, Bruce Townsend, Andrew Moores

Nanometrics Inc. and Daniel McNamara Consulting

PRESENTED AT:

AGU FALL MEETING
New Orleans, LA & Online Everywhere
13–17 December 2021
Poster Gallery brought to you by WILEY

ABSTRACT

Recent scientific applications have increased beyond characterizing earthquake source parameters alone. Seismic stations must record a wide range of earthquake and non-earthquake signals at a high level of fidelity. In this study we compare modeled and observed spectra from earthquakes and non-earthquake sources to instrument self-noise and models of global background signal.

Seismic station and network performance has previously been modeled in terms of detection thresholds and magnitude of completeness for Brune model S-wave spectra (Ackerley, 2012). The spectrum of the peak of the S-wave is used, in order to see if the largest component of the earthquake signal is detectable. However, detecting smaller components of earthquake signal (even from the same source) requires a lower noise threshold. Full waveform analysis requires a reasonable signal-to-noise ratio for smaller amplitude signals throughout the coda. Furthermore earthquakes are not the only signals of interest. Other phenomena such as slow earthquakes, fault creep and tilt, volcanism, water waves, earth normal modes and earthquake gravity produce low amplitude, low frequency signals that challenge the detection capability of seismic stations.

This study compares modeled and observed spectra from earthquake and non-earthquake sources to the self noise of broadband seismometers and standard global background models (NLNM, MLNM, and NHNM). Preliminary results demonstrate the utility of medium-performance portable broadband instruments for standard earthquake studies, and also the importance of low-noise instruments for recording low-power long-period seismic signals from the atmosphere, hydrosphere, cryosphere, and various dynamics of the solid Earth.

REGIONAL EARTHQUAKE MONITORING

Detection and standard analysis of earthquake events (location, time, magnitude estimation etc.) at local and regional distances of 10 km, 100 km, or even out to 3000 km can be well served by a medium performance broadband seismometer (sometimes known as "intermediate band") such as a Trillium Compact, as shown by the figure below.

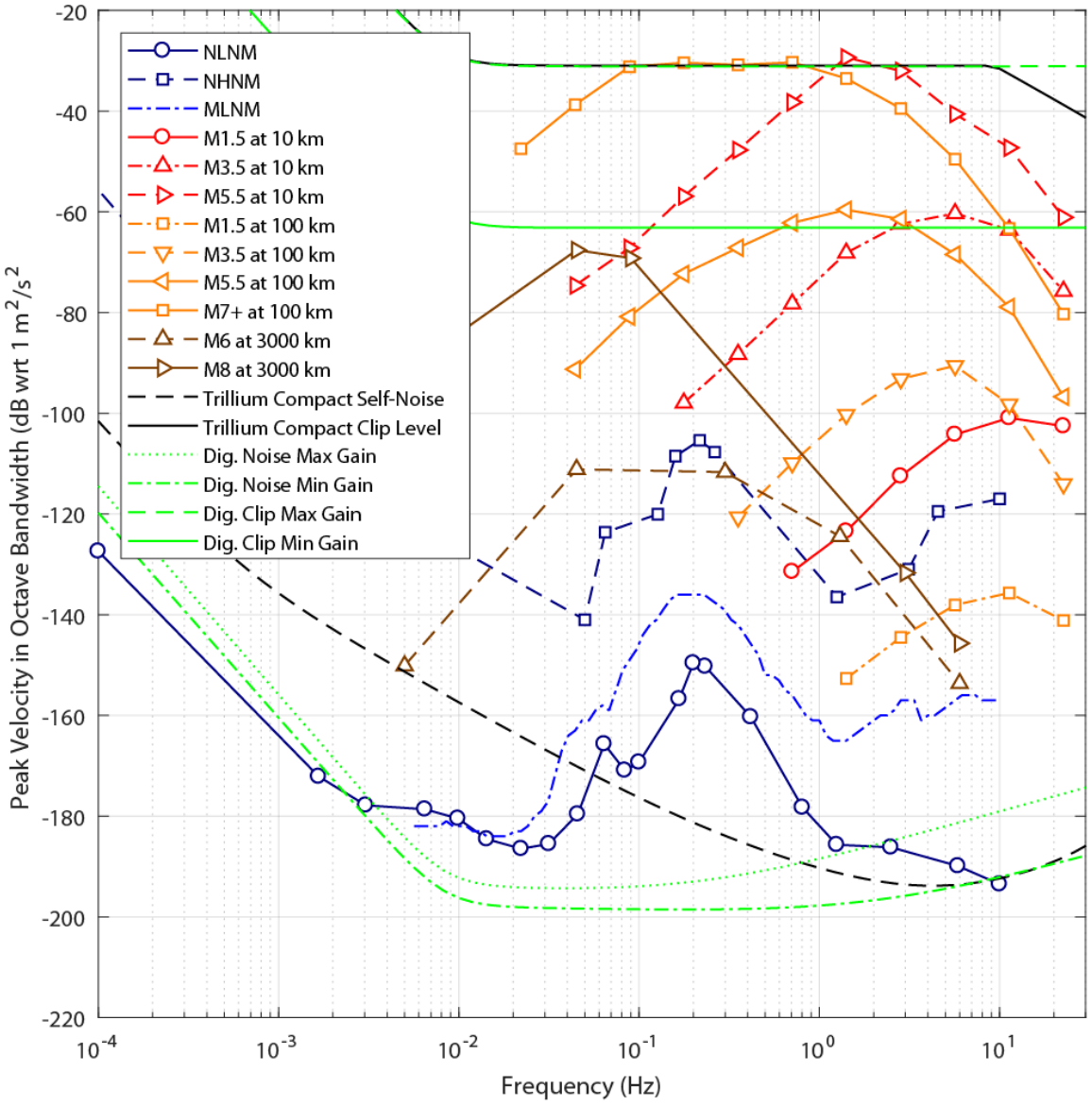

This figure shows the dynamic range of the Trillium Compact 120s seismometer in units of velocity, with clip level (solid black line) at top and noise floor (dashed black line below). Typical earthquake spectra from Clinton and Heaton (2002) are shown for various event magnitudes at distances of 10 km (red lines), 100 km (orange), and 3000 km (brown).

Note these are spectra of the entire earthquake signal, which is dominated by the direct S-wave component. Other components of signal, such as the first break of the P wave or the tail of the coda, will be smaller and have different frequency content.

Clip level is reached only for strong regional events (M7 at 100 km) and moderate local events (M5.5 at 10 km).

High signal-to-noise ratios (SNR) of 50-60 dB are maintained with respect to the instrument noise floor, even for events that are weak (M1.5 at 100 km) or distant (M6 at 3000 km.

Earth background noise is more of a limitation for SNR, as shown by the Peterson (1993) New Low and High Noise Models (NLNM and NHNM) and the McNamara and Buland (2004) Mode Low Noise Model (MLNM), shown in blue. Taking the

MLNM as the most typical seismic background level, we can see this reduces signal-to-noise ratio to approximately 10-20 dB for M1.5 at 100 km and 30-40 dB for M6 at 3000 km. However note that earth background noise drops at low frequencies and falls below the self-noise of the Trillium Compact at frequencies below 0.05 Hz (20 seconds period).

Digitizer noise tends to be relatively insignificant, as shown by the lines near the bottom of the plot indicating noise of the Centaur 24-bit digitizer at 40 Vpp range (dotted green) and 1 Vpp (dash-dot green).

DISTANT EARTHQUAKES

As seismic waves propagate over global distances, higher frequencies become attenuated but signal is still visible below 0.1 Hz (10 seconds period).

The plot below shows the spectrum of a recent M6.5 earthquake at Yilan, Taiwan 2021-10-24 5:11 UT, as received 12,000 km away at Nanometrics test lab in Ottawa, Canada.

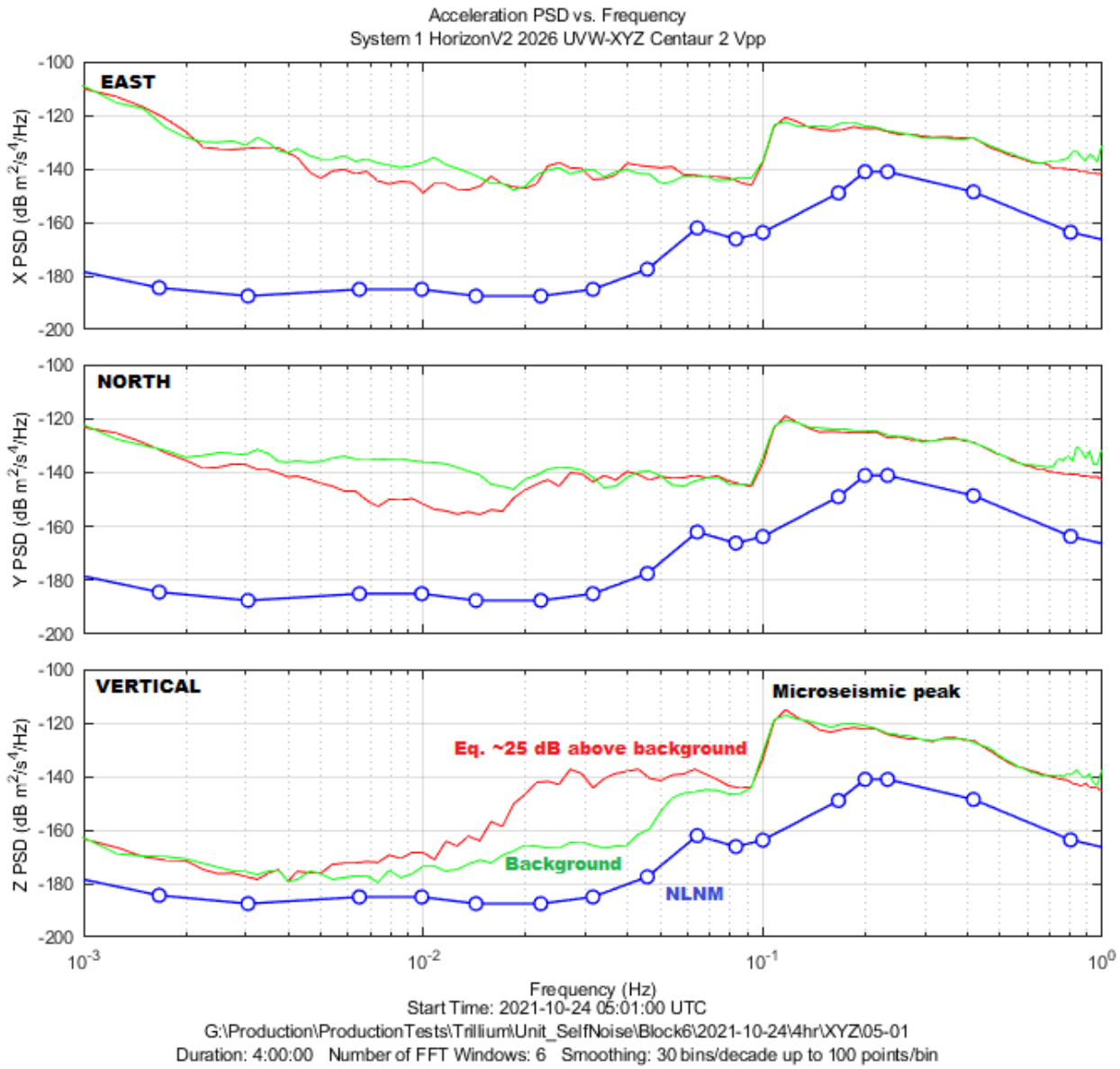

This stacked plot shows low-frequency PSDs of East, North, and Vertical signal as measured by a Trillium Horizon 120 seismometer. Green traces are PSDs of background signal from 1:00-5:00 UT prior to arrival of the earthquake signal, and red traces are PSDs of the next 4 hours 5:00-9:00 containing the earthquake arrival and coda. The earthquake was recorded with about 25 dB SNR on vertical but was not visible on horizontals because of the high level of horizontal tilt noise at this site, a surface pier in a building resting on 15 m of clay.

Since the earthquake signal was below the level of the microseismic peak, filtering was required to see it in a waveform trace. The two figures below show the signal before and after application of a 0.1 Hz lowpass filter.

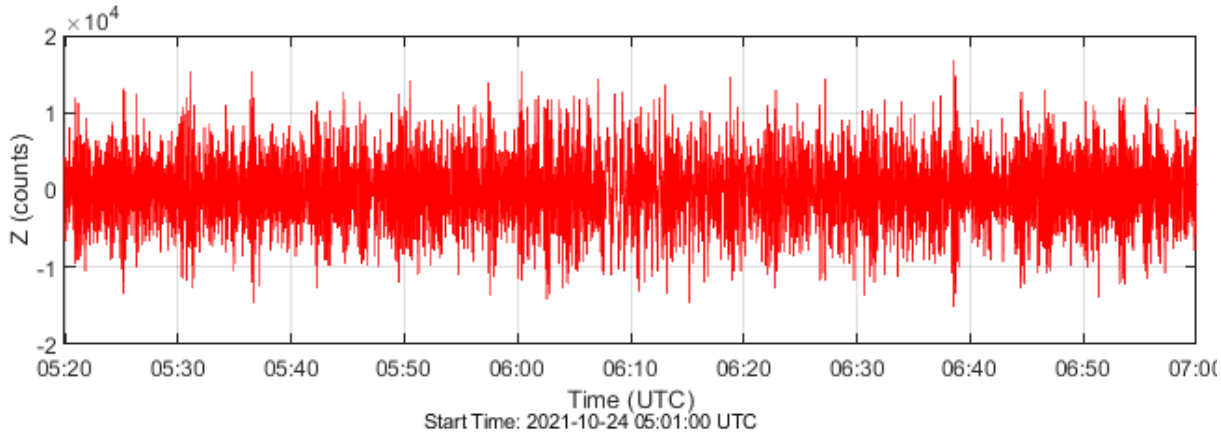

Unfiltered signal, no earthquake visible

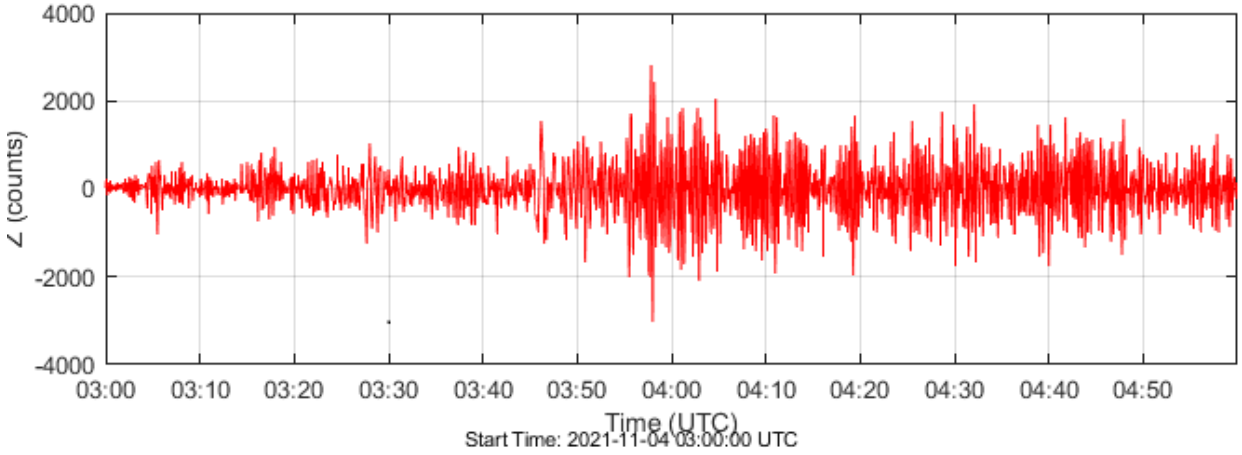

0.1 Hz lowpass, earthquake clearly visible

In this example an M6.5 earthquake was measured at 12,000 km distance with about 25 dB SNR. Since each order of magnitude equals a factor of 10 in amplitude, or 20 dB in signal power, we can infer the threshold of detection would be about M5.3 at this distance, and magnitude would need to be somewhat higher to see the earthquake signal clearly.

This is supported by an example of an M5.7 at Amahai, Indonesia (14,700 km from Ottawa) at 2021-11-04 02:42. The 0.1 Hz lowpass filtered signal from this earthquake is shown below. The earthquake coda is clearly visible, although the SNR is worse and the first break is not clear.

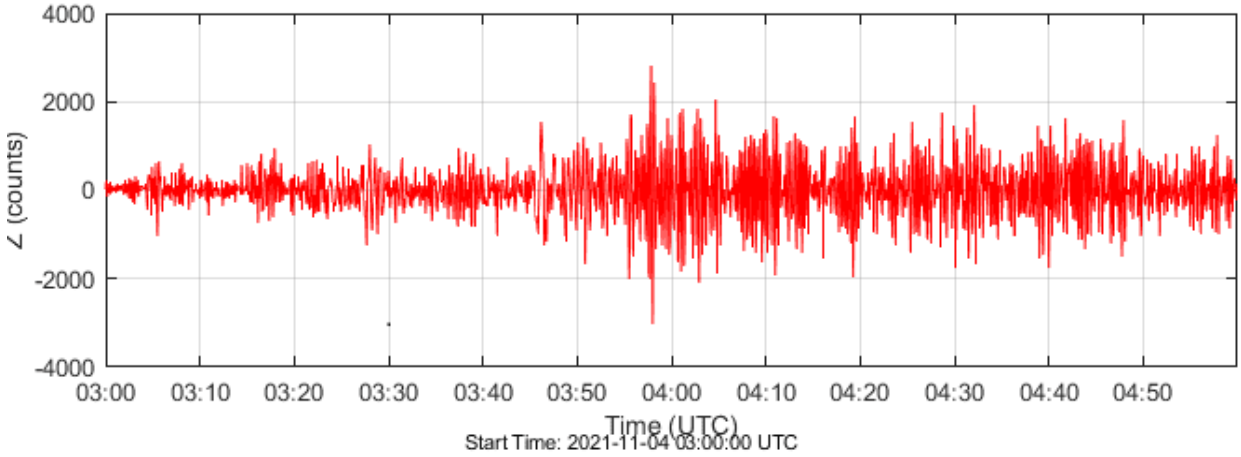

NON-EARTHQUAKE SEISMIC SIGNALS

Volcanism

During an active period at Kilauea, Hawaii in 2011 a series of gas piston events were observed (Choet and Dawson, 2015). Looking back at data from various seismic stations on the island, we can see the resultant ground motion was measured not only near the caldera but throughout the island, for example at IU.POHA, an STS-2 vault station approx. 50 km away. As shown below, these long-period events (10-400 s) spanned several orders of magnitude, but many were small, extending down to the minimum background noise level of -180 dB m/s^2.

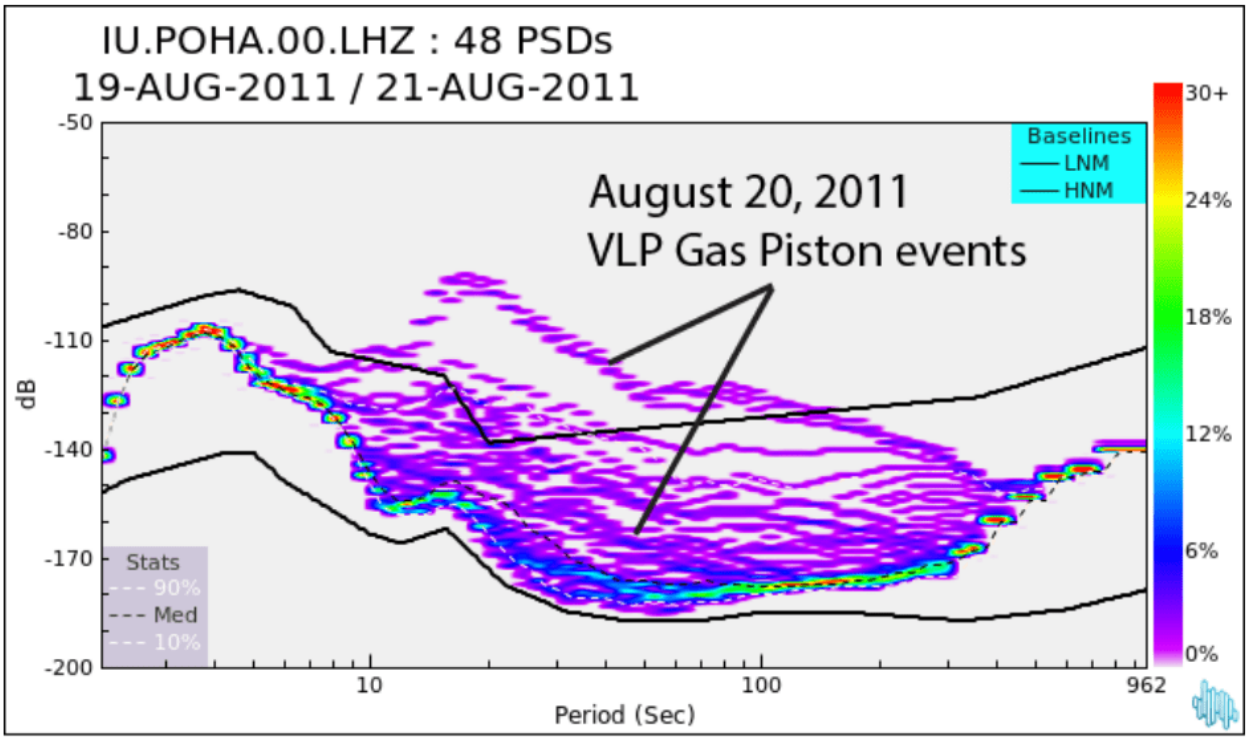

Slow Earthquakes

Authors such as Ide (2007, 2018) have shown that motion across faults ranges continuously in time scale from conventional sudden earthquakes down to nearly continuous creep motion, with a range of frequency content for different events.

Figure 4b below from Matsuzawa (2009) shows an example PSD of a very low frequency earthquake (VLFE) in Japan on 2007-03-15 04:29. It had a slow growth and decay over 1200 seconds, starting near the background noise level (grey line), growing to a peak about 30 dB above background at 0.05 Hz (green lines) and decaying slowly afterwards.

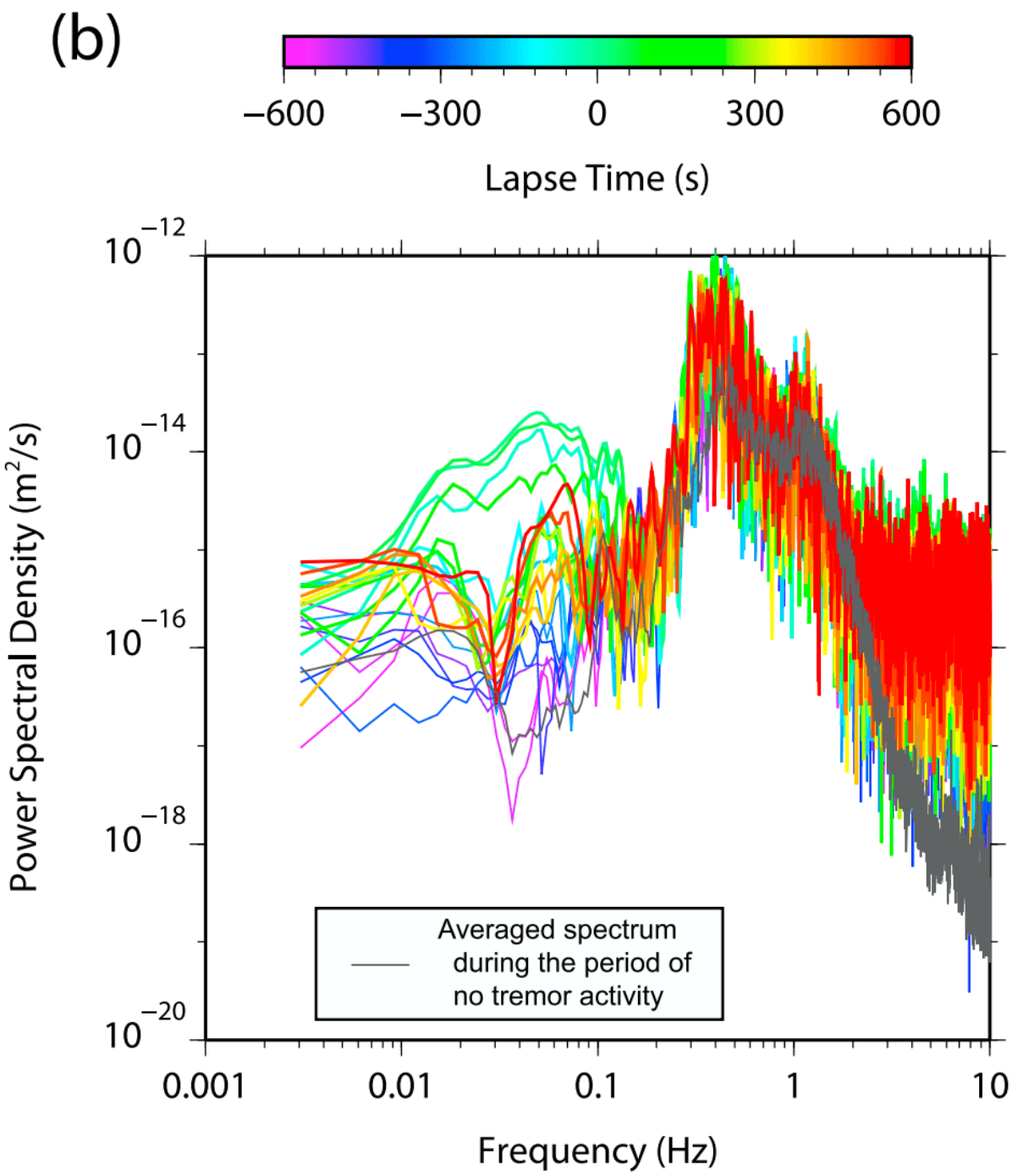

Figure 4. Examples of a velocity seismogram and the power spectra of a VLF at 04:29, 15 March 2007.

The M8.8 earthquake in Bio Bio, Chile at 2010-02-27 6:34 created a tsunami across the Pacific. As it passed Pitcairn Island 5,500 km away the wave height was 20-30 cm, which produced a measurable deflection and tilt of the ground on the island, as seen at GSN station IU.PTCN.

The first figure below shows the direct seismic wave arrival (first red line) about 1000 seconds after the earthquake. The tsunami is not visible in the raw data (top 3 traces) but appears clearly after application of a 100 second lowpass filter (bottom 3 traces). Its arrival time was about 9 hours after the earthquake. The seismic signal was largest on the North component, indicating tilt of the ground in the direction of the seashore to the North of the station.

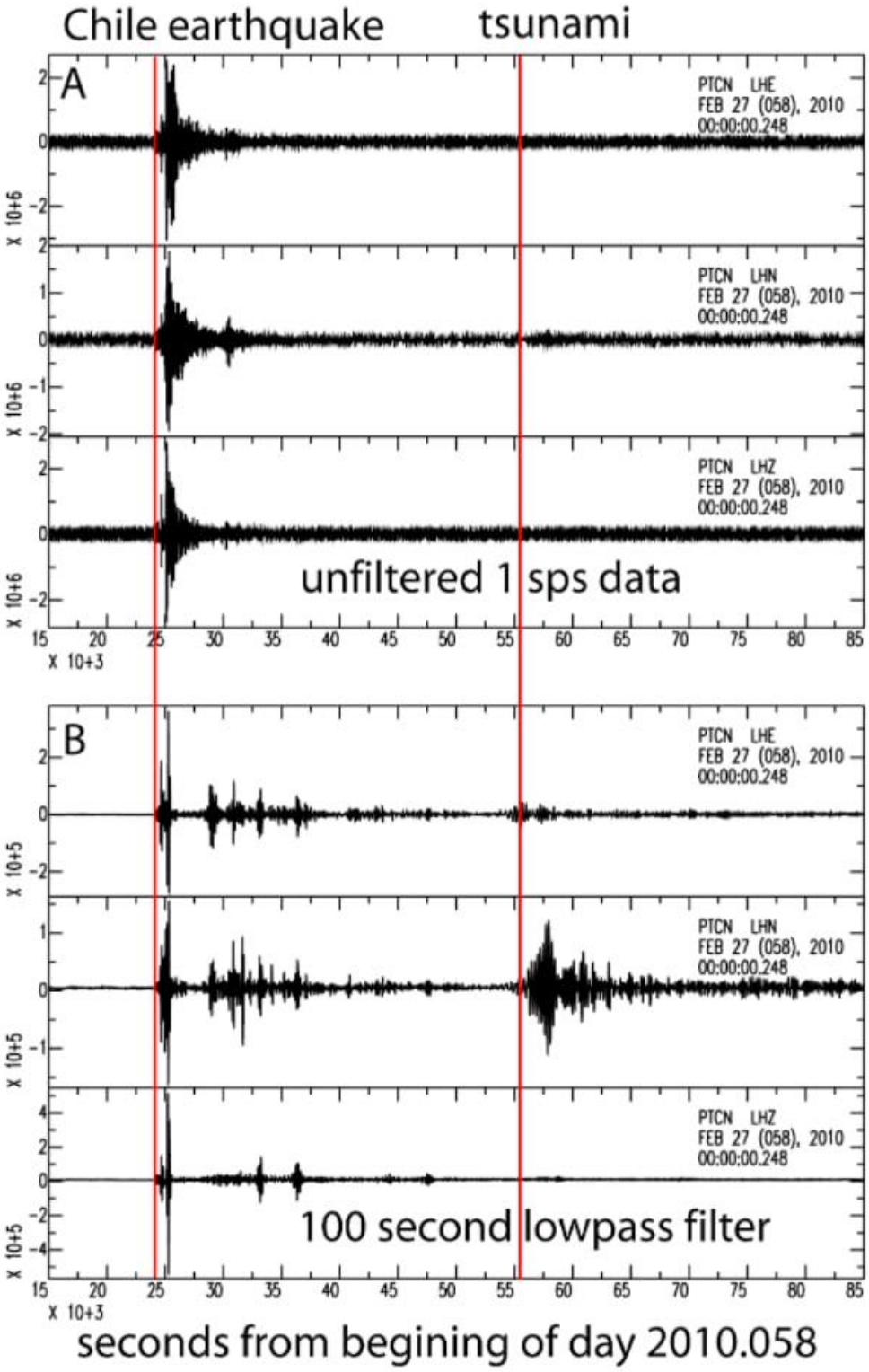

Raw unfiltered 1 sample/second seismic data recorded at Pitcairn Island

The second figure below shows the PSD of the data above, with the earthquake and tsunami visible as two peaks with different amplitude and frequency. The tsunami peaks at 300 seconds period with a SNR of 30 dB.

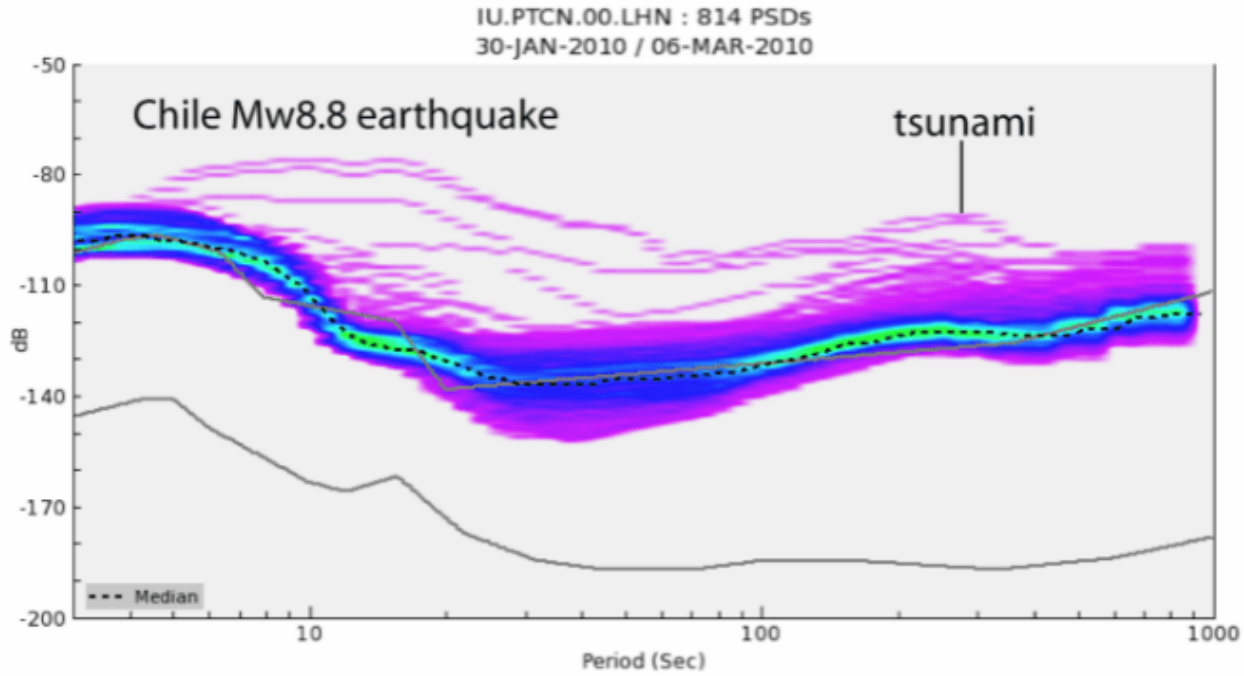

Note the horizontal noise level at this surface vault station is high. A quieter installation such as a borehole or improved vault could potentially reduce the noise and enable detection of smaller events.

Inland waters

The plot below is a composite PSD showing seismic signal at two different sites near bodies of water. Any change in water height due to waves etc. causes measurable deflection of the ground nearby.

The green line shows average background noise at CU.A11 in Canada near the St. Lawrence river, with a peak at 1 second period due to waves on the river. Note this is shorter period (higher frequency) than the secondary microseismic peak caused by ocean waves.

The purple line shows data from CU.BCIP near the Panama Canal, with ground motion due to a seiche (standing wave) peaking in the range of 100-200 seconds (see McNamara et al. 2011).

These water wave effects may be considered either as signals or noise, depending on whether they are of interest for a particular study.

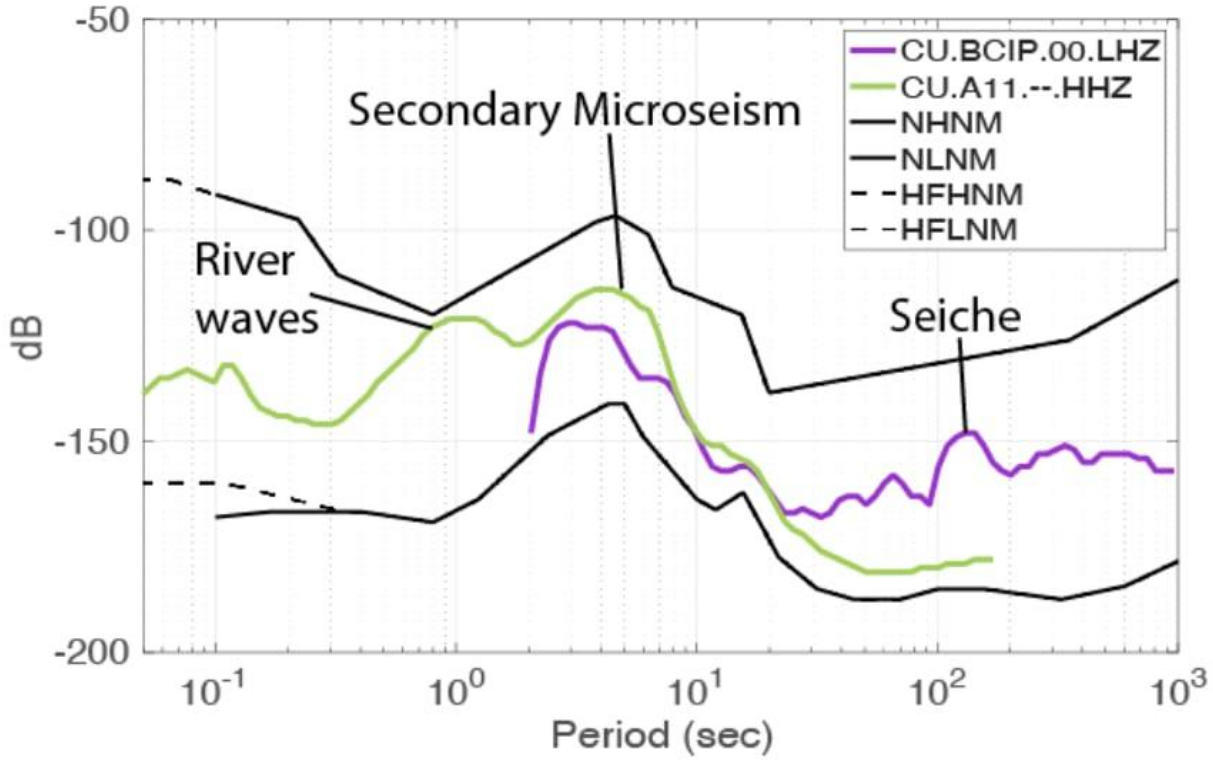

EARTHQUAKE GRAVITY PRECURSOR

Another type of weak long-period signal is the elastogravity effect recently discovered by Vallee et al. (2017). Figure 3 from this paper (below) shows seismic background signal (red lines) at quiet STS-2 sites in Asia. These diverge from the usual zero mean due to a change in gravity as crustal masses shift due to the earthquake. The traces are cut off at the point where the much larger seismic wave signal arrives.

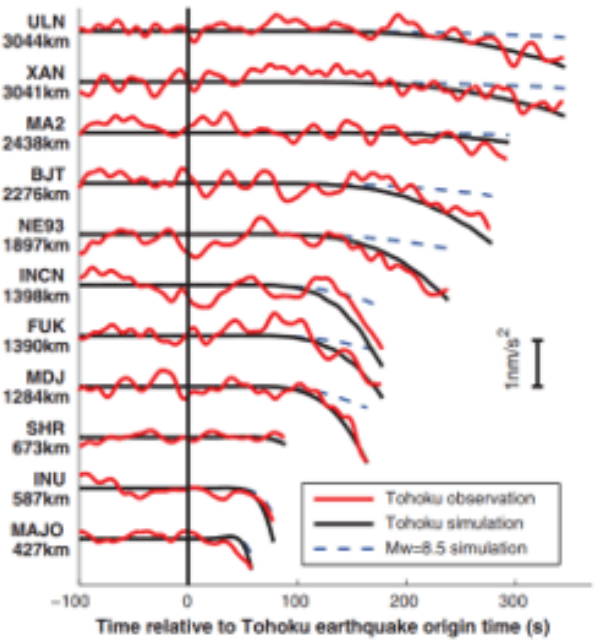

Fig. 3. Agreement between observed and modeled a_z^P signals and influence of the earthquake magnitude. Red (observed) and black (simulated) curves are in good agreement at all distances and azimuths from the Tohoku earthquake. The simulation for a fictitious M_w = 8.5 earthquake (dashed blue curve) shows large amplitude differences, directly illustrating the magnitude determination potential existing in these prompt elastogravity signals.

Vallée *et al.*, *Science* **358**, 1164–1168 (2017) 1 December 2017

It is not practical to calculate a PSD to show the amplitude versus frequency content of this signal, because it is not periodic and is visible for only a short interval. We can roughly estimate frequency content based on rise time (or in this case fall time), where the corresponding wave period T = 2*pi*(rise time).

The rise time ranges from roughly 10 to 100 seconds depending on distance, which corresponds to periods of 60 to 600 seconds, or frequencies of 0.0016 to 0.016 Hz.

Amplitude is difficult to estimate but is clearly not much above background signal levels.

CONCLUSION AND REFERENCES

Conclusion

Seismic installations and studies should be planned with a view towards signal and noise characteristics, to ensure clear recording of all signals of interest. In particular the frequency and amplitude characteristics of the intended signals should inform the choice of instruments, sites, and installation methods. This approach can be applied either retrospectively, choosing appropriate station data for a particular study, or pro-actively, designing a seismic network to ensure recording of signals of future interest.

There is a fundamental limitation on signal to noise ratio in certain bands due to environmental effects, such as the microseismic peak from 0.1 to 1 Hz (1 to 10 s), although this varies from one site to another.

Seismic background levels tend to be lowest in the range of 0.001 to 0.05 Hz (20 to 1000 s), particularly for vertical motion but also potentially for horizontals in a stable installation such as a borehole. This provides a unique window for observation of many geophysical phenomena, not only earthquakes.

Although many phenomena have been observed in this low frequency range, there exist few models of the expected signal characteristics, and nothing comparable to the Brune (1970) model which gives a specific formula for spectra of nearby conventional earthquakes. This preliminary study has surveyed a number of examples of different low frequency seismic phenomena in order to stimulate interest for more comprehensive studies.

References

Ackerley, N. (2012). Estimating the spectra of small events for the purpose of evaluating microseismic detection thresholds. Geo-Convention (pp. 1-10). Calgary: Canadian Society of Exploration Geophysicists.

Ackerley, J.N. and Greig, D.W. (2014) Microseismic Network Performance Estimation Without a Catalogue - Avoiding False Negatives in Traffic Light Protocols; Conference Proceedings, 76th EAGE Conference and Exhibition 2014, Jun 2014, Volume 2014, p.1 - 5

Brune, J. (1970) Tectonic Stress and the Spectra of Seismic Shear Waves from Earthquakes, J. Geophys. Res., Vol. 75, No. 26, pp. 4997-5009.

Chouet, B. and Dawson, P (2015) Seismic source dynamics of gas-piston activity at Klauea Volcano, Hawai"i, Journal of Geophysical Research: Solid Earth 120(4).

Clinton, F. and T. Heaton (2002) Potential Advantages of a Strong Motion Velocity Meter Over a Strong Motion Accelerometer. Seismological Research Letters, Vol. 73 No. 3, pp. 332-342.

Ide, S., Beroza, G.C., Shelly, D.R., Uchide, T. (2007) A scaling law for slow earthquakes, Nature 447(7140): 76-9.

Ide, S. and Maury, J. (2018) Seismic Moment, Seismic Energy, and Source Duration of Slow Earthquakes: Application of Brownian slow earthquake model to three major subduction zones, Geophysical Research Letters 45(7).

Matsuzawa,T., Obara, K., and Maeda, T. (2009) Source duration of deep very low frequency earthquakes in western Shikoku, Japan. Journal of Geophysical Research, Vol. 114, B00A11, doi:10.1029/2008JB006044.

McNamara, D. and R. Buland (2004) Ambient Noise Levels in the Continental United States, Bull. Seism. Soc. Am., Vol. 94, No. 4, pp. 1517-1527.

McNamara, D.E., Ringler, A.T., Hutt, C.R., Gee, L.S. (2011) Seismically observed seiching in the Panama Canal, Journal of Geophysical Research, Solid Earth, Volume 116, Issue B4.

Peterson, J. (1993) Observations and modelling of background seismic noise. Open-file report 93-322, U. S. Geological Survey, Albuquerque, New Mexico.

AUTHOR INFORMATION

Geoffrey Bainbridge, Nanometrics Inc, geoffreybainbridge@nanometrics.ca

Daniel McNamara, Daniel E. McNamara Consulting, daniel.e.mcnamara@gmail.com

Daniela Wuthrich, Nanometrics Inc

Bruce Townsend, Nanometrics Inc

Andrew Moores, Nanometrics Inc

ABSTRACT

Recent scientific applications have increased beyond characterizing earthquake source parameters alone. Seismic stations must record a wide range of earthquake and non-earthquake signals at a high level of fidelity. In this study we compare modeled and observed spectra from earthquakes and non-earthquake sources to instrument self-noise and models of global background signal.

Seismic station and network performance has previously been modeled in terms of detection thresholds and magnitude of completeness for Brune model S-wave spectra (Ackerley, 2012). The spectrum of the peak of the S-wave is used, in order to see if the largest component of the earthquake signal is detectable. However, detecting smaller components of earthquake signal (even from the same source) requires a lower noise threshold. Full waveform analysis requires a reasonable signal-to-noise ratio for smaller amplitude signals throughout the coda. Furthermore earthquakes are not the only signals of interest. Other phenomena such as slow earthquakes, fault creep and tilt, volcanism, water waves, earth normal modes and earthquake gravity produce low amplitude, low frequency signals that challenge the detection capability of seismic stations.

This study compares modeled and observed spectra from earthquake and non-earthquake sources to the self noise of broadband seismometers and standard global background models (NLNM, MLNM, and NHNM). Preliminary results demonstrate the utility of medium-performance portable broadband instruments for standard earthquake studies, and also the importance of low-noise instruments for recording low-power long-period seismic

signals from the atmosphere, hydrosphere, cryosphere, and various dynamics of the solid Earth.

REFERENCES

Ackerley, N. (2012). Estimating the spectra of small events for the purpose of evaluating microseismic detection thresholds. Geo-Convention (pp. 1-10). Calgary: Canadian Society of Exploration Geophysicists.

Ackerley, J.N. and Greig, D.W. (2014) Microseismic Network Performance Estimation Without a Catalogue - Avoiding False Negatives in Traffic Light Protocols; Conference Proceedings, 76th EAGE Conference and Exhibition 2014, Jun 2014, Volume 2014, p.1 - 5

Brune, J. (1970) Tectonic Stress and the Spectra of Seismic Shear Waves from Earthquakes, J. Geophys. Res., Vol. 75, No. 26, pp. 4997-5009.

Chouet, B. and Dawson, P (2015) Seismic source dynamics of gas-piston activity at Klauea Volcano, Hawai"i, Journal of Geophysical Research: Solid Earth 120(4).

Clinton, F. and T. Heaton (2002) Potential Advantages of a Strong Motion Velocity Meter Over a Strong Motion Accelerometer. Seismological Research Letters, Vol. 73 No. 3, pp. 332-342.

Ide, S., Beroza, G.C., Shelly, D.R., Uchide, T. (2007) A scaling law for slow earthquakes, Nature 447(7140): 76-9.

Ide, S. and Maury, J. (2018) Seismic Moment, Seismic Energy, and Source Duration of Slow Earthquakes: Application of Brownian slow earthquake model to three major subduction zones, Geophysical Research Letters 45(7).

Matsuzawa,T., Obara, K., and Maeda, T. (2009) Source duration of deep very low frequency earthquakes in western Shikoku, Japan. Journal of Geophysical Research, Vol. 114, B00A11, doi:10.1029/2008JB006044.

McNamara, D. and R. Buland (2004) Ambient Noise Levels in the Continental United States, Bull. Seism. Soc. Am., Vol. 94, No. 4, pp. 1517-1527.

McNamara, D.E., Ringler, A.T., Hutt, C.R., Gee, L.S. (2011) Seismically observed seiching in the Panama Canal, Journal of Geophysical Research, Solid Earth, Volume 116, Issue B4.

Peterson, J. (1993) Observations and modelling of background seismic noise. Open-file report 93-322, U. S. Geological Survey, Albuquerque, New Mexico.